Adsorption 11: 355–360, 2005

Effects of Activation on the Structure and Adsorption Properties of a Nanoporous Carbon Using Molecular Simulation

SURENDRA K. JAIN* AND JORGE P. PIKUNIC†
Department of Chemical and Biomolecular Engineering, North Carolina State University, Raleigh, NC 27695-7905, USA
skjain2@unity.ncsu.edu

ROLAND J.-M. PELLENQ
CRMCN-CNRS, Campus de Luminy, Case 913, 13288 Marseille Cedex 09, France

KEITH E. GUBBINS
Department of Chemical and Biomolecular Engineering, North Carolina State University, Raleigh, NC 27695-7905, USA

Abstract. We present a study on the effects of activation on a saccharose-based carbon using molecular simulation. A constrained Reverse Monte Carlo method is used to build molecular models that match the experimental structure factors of both activated and unactivated carbon, using appropriate constraints for bond angle and coordination number to describe the three body correlation. The semi-coke sample, that is named CS1000, is obtained by pyrolyzing pure saccharose at 1000°C under nitrogen flow. An activated form of this carbon, CS1000a, was obtained by heating CS1000 in an atmosphere of CO_2 for 20 hours. We built molecular models for CS1000 and CS1000a and also simulated the TEM images of the model. We perform GCMC simulation of a Lennard-Jones model of Argon on the resulting models to obtain the adsorption isotherms. We then study the difference in the morphology of CS1000 and CS1000a that lead to different adsorption properties in carbon upon activation.

Keywords: Reverse Monte Carlo, molecular simulation, activation, adsorption

1. Introduction

Porous carbons are disordered materials with heterogeneous pore structures. They are widely used in industry for separation and purification of gases and liquid mixtures (Sircar et al., 1996) because of their excellent adsorbent properties. The underlying mechanism that leads to adsorption in these materials has been extensively studied. The Surface chemistry of these materials, due to the presence of heteroatoms such as oxygen and hydrogen, plays a major role in adsorption. The adsorption properties of these materials can be greatly enhanced by physical or chemical activation (Marsh et al., 1997). The porous structure of an activated carbon is a strong function of the precursor used in the preparation, and also of the method as well as the extent of activation. During activation certain volatile materials are released which leads to widening of pores, formation of new pores and also an increase in the internal surface area. If chemical activation is used, then certain heteroatoms may also be introduced into the porous material. The efficiency of the activated carbon for polar molecule adsorption depends on the accessible internal volume as well as certain active sites

*To whom correspondence should be addressed.
†Present address: Department of Biochemistry, University of Oxford, South Parks Road, Oxford, UK.

(heteroatoms). Adsorption of nonpolar adsorbates is mostly sensitive to the internal porous structure. In this paper, we concentrate on the structural changes in porous carbons brought about by activation. We also explore the activation effects on argon adsorption.

The texture and micro-structure of porous carbons cannot be determined from experiment at the present time. Thus, a suitable model for the internal structure of carbon is required to predict adsorption and diffusion properties. To that purpose, models that describe the pore structure in the porous carbons in a realistic way have to be developed. Many models have been proposed in the last few years and have been recently reviewed (Bandosz et al., 2003). In previous works (Pikunic et al., 2002, 2003), a reconstruction procedure based on constrained Reverse Monte Carlo (RMC) was used to generate atomistic models that quantitatively match experimental (diffraction and small angle) properties of two real porous saccharose cokes, CS400 (density $\sim$1 g/cm^3) and CS1000 (density $\sim$1.5 g/cm^3), heat treated at 400° and 1000°, respectively. In this work, we apply the same procedure to develop a molecular model for an activated CS1000 sample, which we call CS1000a. We also simulate TEM images of the resultant model. Finally, we discuss the structural differences between CS1000 and CS1000a by comparing the result we obtained in this work to that obtained for CS1000 in a previous work (Pikunic et al., 2003). We also compare the adsorption properties of both models using GCMC simulations.

2. Simulation Methods

2.1. Reverse Monte Carlo

The Reverse Monte Carlo (RMC) method was initially proposed by McGreevy and Pustzai (1988). The idea is to generate an atomic configuration of a system that matches the structural properties of the real system obtained by experiment. Throughout the simulation the differences between the simulation and experimental structural properties are minimized. The most commonly used structural property in RMC methods is the structural factor, $S(Q)$ and the quantity to be minimized is

$$\chi^2 = \sum_{i=1}^{n_{\exp}} [S_{\text{sim}}(q_i) - S_{\exp}(q_i)]^2 \qquad (1)$$

where S_{sim} is the simulated structure factor and $S_{\exp}$ is the experimental structure factor. The probability of acceptance of a new atomic configuration is given by

$$P_{\text{acc}} = \min\left[1, \exp\left\{-\frac{1}{T_\chi}\left(\chi^2_{\text{new}} - \chi^2_{\text{old}}\right)\right\}\right] \qquad (2)$$

where T_χ is a weighting parameter.

The uniqueness of structures determined by the RMC method has been questioned in the literature (Evans, 1990). If many body forces are important in a system then we need to include some constraints, representative of these forces, in the RMC method to completely specify the system. We have developed appropriate constraints for the porous carbons in a previous work (Pikunic et al., 2002). We use the same constraints in this work to build a molecular model for CS1000a. These constraints are:

$$\begin{aligned}
\chi^2 &= \sum_{i=1}^{n\exp} [g_{\text{sim}}(r_i) - g_{\exp}(r_i)]^2, \\
\delta^2 &= \left[\left(\frac{N_3}{N}\right)_{\text{sim}} - \left(\frac{N_3}{N}\right)_{\text{target}}\right]^2, \\
\psi^2 &= \frac{1}{n}\sum_{\theta_i=1}^{n_\theta}\left[\cos(\theta_i) - \cos\left(\frac{2\pi}{3}\right)\right]^2
\end{aligned} \qquad (3)$$

2.2. Reverse Monte Carlo in the Simulated Annealing Framework

Simulated annealing is a minimization technique (Kilpatrick, 1983) based on the analogy between minimizing a cost function in a combinatorial optimization problem and the slow cooling of a solid. The simulated annealing method consists of first melting the solid to be optimized at a higher temperature and then slowly lowering the temperature. The system is allowed to equilibrate at each temperature. The temperature is lowered until no further change in the structure is observed. In the simulation we simultaneously minimize the cost functions χ^2, ψ^2 and δ^2. More details can be found in Pikunic et al. (2002). The simulation is carried out in a cubic box with periodic boundary conditions. The number of carbon atoms in the box remains constant during the simulation and corresponds to the experimental density. Starting from a random initial configuration and at a high temperature, we randomly select an atom and displace it randomly to a new position. The system runs at this temperature for a number of moves and is allowed to come to equilibrium. The temperature is then lowered by multiplying T_χ with a constant between 0 and 1. The simulation is completed when no significant

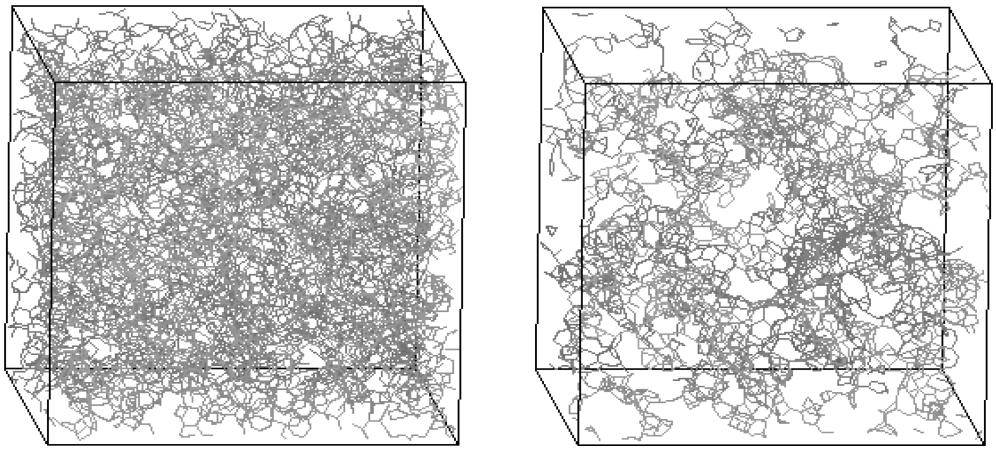

Figure 1. Snapshot of the resultant model of CS1000 (left, Pikunic et al., 2003) and CS1000a (right, this work). The rods represent C-C bonds. The box size is 5 nm.

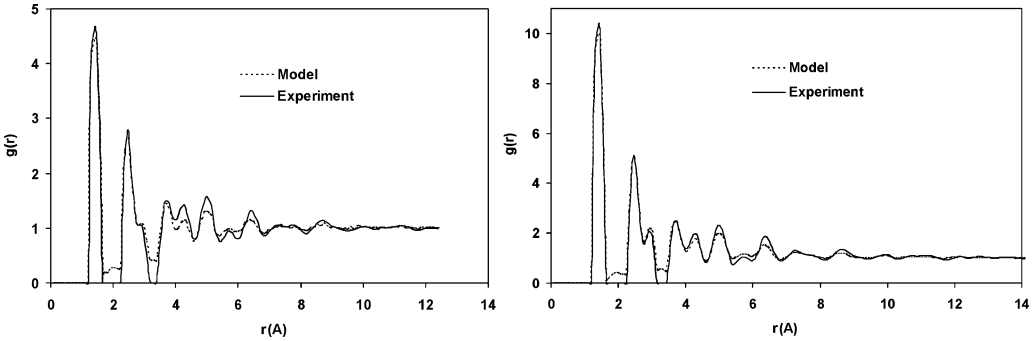

Figure 2. Comparison of pair correlation functions obtained from MCGR method (solid line) and the RMC method (dashed line) for CS1000 (left, Pikunic et al., 2003) and CS1000a (right, this work).

changes in the three cost functions to be minimized are observed.

3. Results and Discussion

The initial semi coke sample was obtained by pyrolizing pure saccharose at 1000°C under nitrogen flow. This was named CS1000. Another sample, CS1000a, was obtained by the activation of CS1000. The activation was carried out by heating CS1000 in a CO_2 atmosphere for 20 hours. From experiments, the density of carbon atoms in CS1000 was obtained as 1.584 gm/ml and that of CS1000a as 0.722 gm/ml. We built a molecular model for CS1000a using our simulation protocol in a 5 nm box. The number of atoms to be placed in the simulation box was calculated from the measured density. We monitored the three cost functions throughout the simulation. The three cost functions do not change initially, but as we quench the system, the three cost functions start decreasing. The simulation was completed when no further changes in the three cost functions was observed. A snapshot of the final configuration of CS1000a along with CS1000 is shown in Fig. 1.

As can be seen from Fig. 1, both models represent very disordered structures. CS1000a, the activated carbon, has comparatively low density and large pores. The simulated and experimental radial distribution functions, shown in Fig. 2, are in good agreement. The comparison between the pair correlation functions of CS1000 and CS1000a reveal that CS1000a is more ordered than CS1000 which is evident from the fact that the peaks of CS1000a are more pronounced. This is not surprising since activation is known to produce more ordered structures by removing the volatile gaseous materials. The residue elementary carbon atoms are

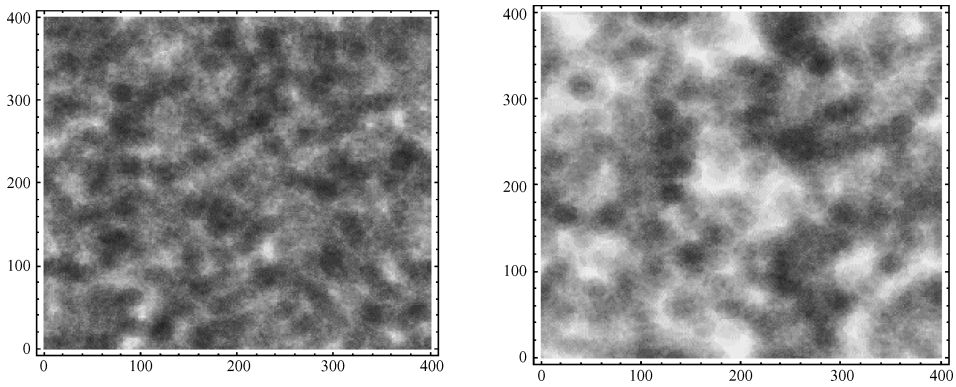

Figure 3. Simulated TEM images of CS1000 (left, Pikunic et al., 2003) and CS1000a (right, this work).

then grouped into stacks of flat aromatic sheets cross linked in a random manner (Marsh et al., 1997). Integration over the first peak of the pair correlation function gives the first coordination number for the carbon atoms. The coordination number for CS1000a is found to be 2.89 and that for CS1000 is 2.77. Thus, we believe CS1000a has a more graphite-like structure. To further compare the structural difference of the two models, we simulated the TEM images for the model CS1000a and compared it with that of CS1000, which we reported in a previous work. The details of TEM simulation can be found elsewhere (Pikunic et al., 2003). We assume that the diffraction contrast is negligible compared to mass-thickness contrast. We present the simulated TEM images of CS1000a and CS1000 in Fig. 3.

The density of the darker regions, which is related to the amount of matter that appears in the simulated TEM images, is large for CS1000 as compared to CS1000a. Moreover, the white regions in the simulated TEM images, which represent the pores, are large in dimension for CS1000a as compared to CS1000. This indicates that CS1000a has a higher porosity and that the pores are larger than those in CS1000.We calculated the pore size distribution (PSD) using a method similar to that suggested by Gelb and Gubbins (1998). The PSD, $p(H)$, is defined by $p(H)$ dH, the fraction of pore volume that is occupied by pores in the range H and $H + dH$. Figure 4 shows the pore size distribution for both models. From the above figure we can see that CS1000a has a broad distribution with a maximum pore size of nearly 12 Å. The distribution for CS1000 is comparatively narrow and a large fraction of pores are in the small micropore range (3.5–5.0 Å). This is consistent with the observation from TEM images that CS1000a has wide micropores. We also calculated the porosity of CS1000 and CS1000a using argon as a test particle. The porosity of CS1000 and CS1000a was found at 0.068 and 0.568 respectively.

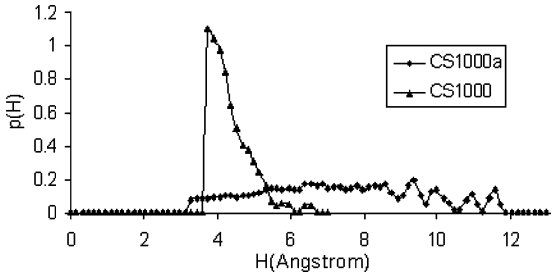

Figure 4. Pore size distribution of CS1000 (Pikunic et al., 2003) and CS1000a (this work).

In a recent work we calculated the adsorption isotherm of argon in CS1000 at 77.4 K (Pikunic et al., 2004). Here we calculated the adsorption isotherm of argon at 77.4 K in the model CS1000a using GCMC simulations. The details of the GCMC simulations can be found elsewhere (Frenkel and Smit, 2002). Argon is modeled as a simple Lennard Jones fluid. The interaction parameters used in the simulation are given in Table 1 (Pikunic et al., 2004). Type I reversible isotherms were obtained for both the models. The adsorption isotherms are shown in Fig. 5. The adsorption

Table 1. LJ potential parameters for Carbon-Argon and Argon-Argon interactions.

Interaction pair	σ (in Angstrom)	ε/K_B (in Kelvin)
Carbon-Argon	3.38	58.0
Argon-Argon	3.405	120.0

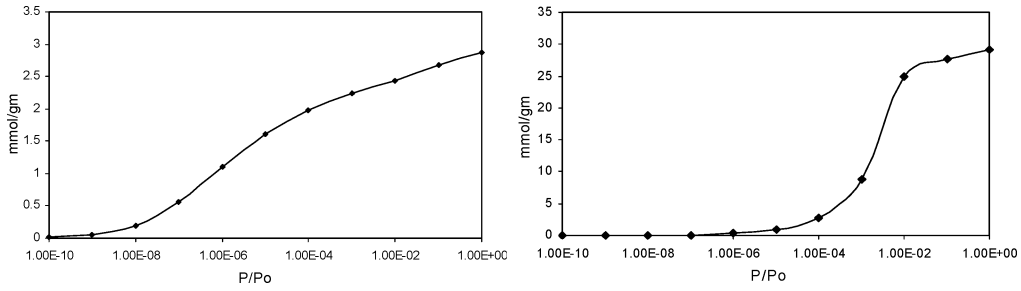

Figure 5. Argon adsorption isotherms at 77.4 in the models of CS1000 (Pikunic et al., 2004) (left) and CS1000a (right).

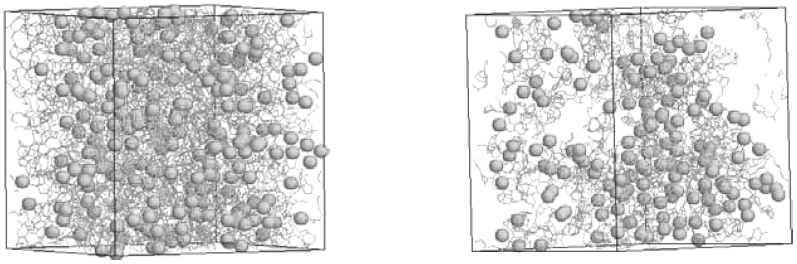

Figure 6. Snapshot of Argon adsorption in CS1000 (left) and CS1000a (right) at $P/P_0 = 0.001$.

isotherm for activated carbons are typically of Type I, IV or V (Gregg and Sing, 1982).

Figure 5 (the x-axis has been plotted in log scale for clarity) shows that both CS1000 and CS1000a has a Type I isotherm, which is characteristic of microporous carbons. In microporous solids, adsorbate molecules experience a strong attractive force due to the overlap of the interaction potentials from the opposing pore walls and this force is a strong function of the pore width. This results in an initial steep slope in the adsorption isotherm at low pressures. Adsorption in CS1000a starts at relatively large pressures as seen from Fig. 5. This can be attributed to the relatively large pores in CS1000a, where the fluid-wall interaction is not as strong as that in CS1000. There is a significant rise in the adsorption isotherm of CS1000a from $P/P_0 = 0.001$ to 0.01 as can be seen from Fig. 5. We show a snapshot of argon adsorption in CS1000 and CS1000a Fig. 6 at $P/P_0 = 0.001$. We can see that the pores of CS1000 are almost saturated whereas CS1000a has some large pores which are only partially filled. The loading capacity of CS1000a is nearly 10 times that of CS1000 which is mainly due to the different pore size distributions in the two models as well as due to the low density of CS1000a sample.

The large porosity of CS1000a can be due to pore opening (opening of blocked pores) and pore widening, or due to the formation of more micropores (Kennedy et al., 2004). The analysis of TEM, PSD and adsorption data provides ample evidence that activation of CS1000 results in wide micropores in CS1000a. This might be a result of widening of the already existing pores in CS1000 or creation of new pores in the wide micropore range. We have calculated the isosteric heat of adsorption for CS1000 (Pikunic et al., 2004); quantitative agreement with experiment was obtained. We are currently carrying out simulations to calculate the isosteric heat for argon in CS1000a. Comparing the fluid-fluid and fluid-wall interaction at different loadings for CS1000 and CS1000a will give us further insight into the structural heterogeneity of the two models, and will also help us to better understand the adsorption behavior.

Acknowledgments

We thank Isabelle Rannou, Nathalie Cohaut and Jean Michel Guet (CRMD, Orléans, France) for providing us the X-ray, SAXS and density results. We also thank Henry Bock, Benoit Coasne and Erik Santiso for helpful discussions. This work was funded by the National Science Foundation, through the grant CTS-0211792.

References

Bandosz, T.J., M.J. Biggs, K.E. Gubbins, Y. Hattori, T. Liyama, K. Kaneko, J. Pikunic, and K. Thomson, "Molecular Models of Porous Carbons," *Chemistry and Physics of Carbon*, L.R. Radovic (Eds.), Vol. 28, pp. 137–199, Marcel Dekker, New York, 2003.

Evans, R., "Comment on Reverse Monte Carlo Simulation," *Mol. Simul.*, **4**, 409–411 (1990).

Frenkel, D. and B. Smit, *Understanding Molecular Simulation 2nd Ed.*, pp. 126–132, Academic Press, New-York, 2002.

Gregg, S.J. and K.S.W. Sing, *Adsorption, Surface Area and Porosity 2nd Ed.*, pp. 3–12, Academic Press, London, 1982.

Gelb, L.D. and K.E. Gubbins, "Pore Size Distribution in Porous Glasses: A Computer Simulation Study," *Langmuir*, **15**, 305–308 (1999).

Kennedy, L.J., J.J. Vijaya, and G. Sekaran, "Effect of Two-Stage Process on the Preparation and Characterization of Porous Carbon Composite from Rice Husk by Phosphoric Acid Activation," *Ind. Eng. Chem. Res.*, **43**, 1832–1838 (2004).

Kilpatrick, S., "Optimization by Simulated Annealing," *Science*, **220**, 671–680 (1983).

Marsh, H., E.A. Heintz, and F. Rodriguez-Reinoso, *Introduction to Carbon Technologies*, University of Alicante, 1997.

McGreevy, R.L. and L. Pustzai, "Reverse Monte Carlo Simulation: A New Technique for the Determination of Disordered Structures," *Mol. Simul.*, **1**, 359–367 (1988).

Pikunic, J., C. Clinard, N. Cohaut, K.E. Gubbins, J.M. Guet, R.J.-M. Pellenq, I. Rannou, and J.N. Rouzaud, "Reconstruction Method for the Characterisation of Porous Carbons," *Stud. Surf. Sci. Catal.*, **144**, 19–26 (2002).

Pikunic, J., C. Clinard, N. Cohaut, K.E. Gubbins, J.M. Guet, R.J.-M. Pellenq, I. Rannou, and J.N. Rouzaud, "Structural Modeling of Porous Carbons: Constrained Reverse Monte Carlo Method," *Langmuir*, **19**(20), 8565–8582 (2003).

Pikunic, J., P. Llewellyn, R. J-M. Pellenq, K. E. Gubbins, *Langmuir*, submitted, 2004.

Sircar, S., T.C. Golden, and M.B. Rao, "Activated Carbon for Gas Separation and Storage," *Carbon*, **34**(1), 1–12 (1996).